Journal of Applied Electrochemistry **31**: 1339–1344, 2001.

Electrochemical monitoring of water remediation by metallic iron

T. BIGG and S.J. JUDD*
School of Water Sciences, Cranfield University, Cranfield, Bedfordshire, UK
*(*author for correspondence, fax: +44 (0)1234 751671, e-mail: s.j.judd@cranfield.ac.uk)*

Received 21 May 2001; accepted in revised form 27 July 2001

Key words: dyewaste, metallic iron, Nernst, oxidation reduction potential

Abstract

Oxidation reduction potential (ORP) changes were monitored during the course of the remediation of four wastewater matrices by metallic iron (Fe^0) based on a batch fluidized bed reactor. Two of these matrices contained azo dyes (Acid Orange II and Acid Blue 113), another contained pentachlorophenol and the fourth was an authentic dyewaste. For the azo dye Acid Orange II ORP was found to follow the same trend as the dye concentration ([AOII]), decreasing exponentially with time over the course of the remediation. Change in ORP was found to be directly proportional to [AOII] and to follow a logarithmic relationship with $[Fe^{2+}]^2[aa]^2[AOII]^{-1}$, indicating a Nernstian behaviour. It is concluded that the ratio of remediation products to reactants can be determined directly by monitoring changes in ORP. The electrochemical conditions that influence corrosion were found to control remediation, consistent with the remediation being driven by anaerobic corrosion and predicted from potential–pH Pourbaix diagrams.

1. Introduction

1.1. *Background*

Reductive chemical treatment of wastewater by metallic iron shows much promise for sequestration of certain metal oxy-anions [1] and organic pollutants [2–9]. It is inexpensive to obtain [10] and offers clear advantages over conventional treatment methods [11], especially as an alternative to oxidative treatment by more hazardous and costly chemical reagents. Understanding the nature of remediation by metallic iron represents an important step in expediting its more widespread adoption.

As with all solid–liquid contacting reactors, the process takes place by transfer of the pollutant from bulk solution to the iron metal surface followed by chemical reaction at the solid–liquid interface. The overall process has been shown, from studies of a fluidized bed system, to be mass transfer-limited [12]. In the absence of oxygen the second stage is driven by anaerobic corrosion of the iron metal [13, 14], and the e.m.f. of the overall reaction provides the driving force for the reductive degradation reaction coupled with the corrosion of the iron [10]. It is this chemical component of the remediation process that is investigated in this paper.

Four wastewater analogues have been investigated: two azo dyes (Acid Orange II and Acid Blue 113), a common industrial effluent organic pollutant (pentachlorophenol, PCP) and an actual dye-house waste concentrate. Azo dyes were initially chosen since they (a) contribute to colour contamination in dyehouse effluents, (b) are readily degraded by metallic iron under anaerobic conditions, and (c) can be monitored as readily as the oxidation reduction potential (ORP). The abiotic reduction of azo linkages in environmental media has been inferred from experiments with anaerobic sediments [15–17] but the complexity of this system makes it difficult to fully characterize the processes involved [18]. An additional advantage of investigating azo dye colour remediation is that it provides insight into azo linkage destruction by metallic iron. Acid Orange II, which has been employed in similar studies [12, 19, 20] forms the main analogue used in this investigation.

1.2. *Equilibrium thermodynamics*

The chemical reaction between a dye (e.g., Acid Orange II) and metallic iron is represented by

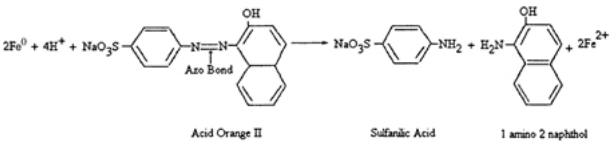

(1)

Based on Nernst theory the change in ORP arising from the above reaction at is given by

$$\Delta\mathrm{ORP} = \frac{RT}{zF}\log\frac{[\mathrm{Fe}^{2+}]_t^2[\mathrm{aa}]^2}{[\mathrm{Dye}]} \quad (2)$$

where R is the gas constant, T the absolute temperature, z the number of charges transferred and F the Faraday constant. [aa] refers to the concentration of aromatic amine products and relates to $([\mathrm{Dye}]_0 - [\mathrm{Dye}]_t)$, and $[\mathrm{Dye}]_0$ and $[\mathrm{Dye}]_t$ refer to the dye concentration initially and at time t. Assigning Q to the logarithmic term and putting $z = 2$ and $T = 293.15$ produces the simplified expression:

$$\Delta\mathrm{ORP} = 29.1 \log Q \quad (3)$$

2. Experimental details

2.1. *Materials*

The experimental fluidized bed rig is illustrated in Figure 1 and detailed in Table 1. The water contaminants investigated are listed in Table 2. All laboratory-produced solutions were made up with 1.0 MΩ deionized water. The dyehouse concentrate derived from a dyewaste processing and water recovery plant (T. Forsell, Leics.) in which reverse osmosis is used to remove and concentrate the dissolved components in the dyewaste stream. The metallic iron employed throughout these remediation reactions was >90%-pure iron metal powder (P&R Laboratory Supplies Ltd, St Helens). Samples were fractionated to 40–53 μm using Endecott sieves and degreased to remove any adhering grease layer. All iron powder was discarded at the end of each run and virgin material used throughout.

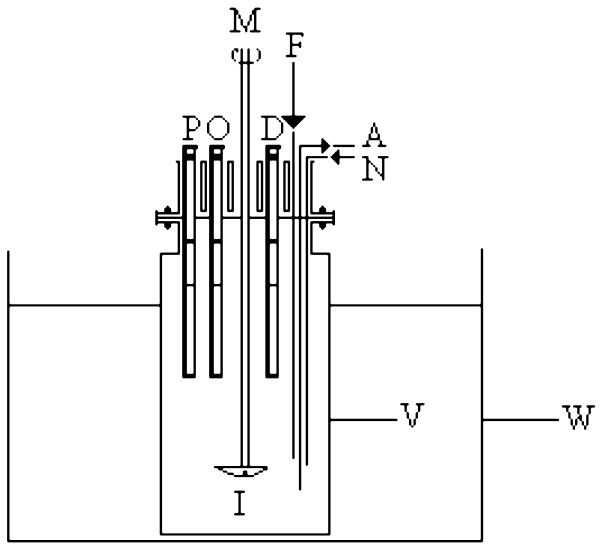

Fig. 1. Schematic diagram of the fluidized bed system. Key: (A) sampling point; (D) dissolved oxygen electrode; (I) four pitch blade impellor; (M) overhead mixer; (N) nitrogen gas purge; (O) oxidation–reduction potential electrode; (P) pH electrode; (V) reactor vessel; (W) water bath.

Table 1. Reactor parameters

Parameters	Values
Reactor type	Fluidized bed
Reactor volume	5.4 l
Dissolved oxygen	0 mg l^{-1}
Iron pretreatment	Degreasing with methylated spirits and ethanol for one minute
Temperature in reactor	293 ± 1.3 K
Mixing speed	33.3 ± 0.1 revolutions per second
Iron concentration	23 150 mg l^{-1}
Fe^0 mean particle size	46.5 μm
Fe^0 specific surface area	0.5 to 1.0 $m^2 g^{-1}$
Impellor diameter	57 mm

Table 2. Analogues

Contaminant	Spectrophotometric analysis	Supplier
Acid Orange II	486 nm	Sigma
Acid Blue 113	567 nm	Clariant UK
Pentachlorophenol	Full UV spectrum	BDH
Concentrated dyewaste constituents	Full visible spectrum	T. Forsell

2.2. *Methods*

Remediation reactions were carried out under the base conditions described in Table 1. The reaction was monitored spectrophotometrically using a Jenway 9605 UV/Vis spectrophotometer depending on the water contaminant being investigated. Baseline recordings and calibrations were obtained with deaerated buffer solution filtered through 1 g glass wool (Fisher, Loughborough). Spectral and photometric analyses were performed immediately upon extraction from the reactor to prevent interference from oxidation of Fe^{2+} to Fe^{3+}. Concentrations were calculated from absorbance readings using absorbance–concentration calibration graphs constructed according to Beer's law. All experiments were replicated at least four times. Pentachlorophenol was additionally assayed by GC-MS (HSL, Sheffield).

The ORP was recorded using a Jenway 3340 ion meter fitted with a platinum redox/ORP electrode. Calibration of this electrode was carried out with reference to a Ag/AgCl 200 mV redox standard solution before and at the end of individual runs. pH was measured using a combined pH/reference electrode fitted to the ion meter, and the probe was calibrated with pH 4, 7 and 10 buffers (BDH, Lutterworth) before and after each run to ensure consistent calibration. pH values of the solutions under investigation were adjusted by addition of appropriate buffers (Table 3). Remediation of Acid Orange II was investigated under a range of pH conditions. Fe^{2+} analysis was carried out on solution samples extracted

Table 3. Buffers

pH	Buffer chemical	Supplier
1.4	0.04 M KCl 0.0332 M HCl	BDH
3.1	0.0411 M Na_2HPO_4 0.07945 M citric acid	BDH
4.5	0.0935 M Na_2HPO_4 0.05325 M citric acid	BDH
5.8	0.0035 M HEPES	Aldrich
7.0	0.1647 M Na_2HPO_4 0.01765 M citric acid	BDH
9.6	0.1 M Na_2HPO_4	BDH

during the course of reaction using a Thermo Jarrell Ash ICP-AES interfaced with Atomscan computer software. The spectrometer was calibrated using 1 to 1000 mg l^{-1} standards in 0.5% nitric acid matrix.

Dissolved oxygen (DO) concentration was monitored using a Jenway 9300 meter, which was pre-calibrated before each run. Prior to each run DO levels were reduced to 0 mg l^{-1} by purging with oxygen-free nitrogen gas (BOC, Oxon) supplied at 0.5 bar until a steady reading of 0 mg l^{-1} had been obtained for one hour prior to the commencement of each run. Temperature was kept constant using a thermostatically-controlled water bath and recorded by means of a temperature sensor connected to the DO electrode.

3. Results

3.1. *Equilibrium thermodynamics*

Figure 2 shows the ORP as a function of Acid Orange II dye concentration (C_{AOII}) over the course of the remediation reaction. The data points each represent an average of five replicate experiments and the error bars shown indicate a precision of ±15%.

Both ORP and C_{AOII} were observed to alter logarithmically with time according to the empirical relationships:

$$\mathrm{ORP(mV)} = -73.075 \times \ln(\mathrm{minutes}) + 40.614 \qquad R^2 = 0.997$$

$$C_{AOII}(\mathrm{mg\,l^{-1}}) = -1.7623 \times \ln(\mathrm{minutes}) + 3.596 \qquad R^2 = 0.963$$

The change in ORP thus varies linearly with dye concentration:

$$\Delta\mathrm{ORP} = 8.7 \times 10^6 \times C_{AOII} - 197 \quad (4)$$

For every mole of AOII destroyed in the remediation reaction 12 moles of Fe^{2+} were produced, representing a six-fold stoichiometric excess according to Equation 1.

The correlation of ΔORP with $\log Q$ is linear (Figure 3). The Figure includes the theoretical line given by Equation 3, based on data from the assay of both dye and dissolved iron, clearly indicating the Nernstian behaviour being exhibited during the remediation reaction.

3.2. *Effect of pH*

Pseudo first order reaction rate constants (k) for the remediation of Acid Orange II were obtained at six different pH values (Figure 4), and the following correlation obtained:

$$k = 8.1086\,\mathrm{e}^{-0.483\,\mathrm{pH}} \qquad R^2 = 0.96 \quad (5)$$

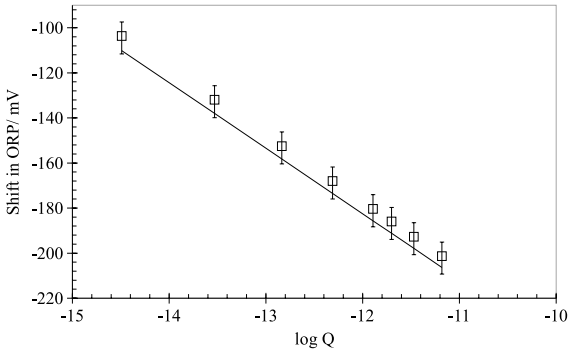

Fig. 3. ΔORP against Q, Acid Orange II remediation. Key: (□) experimental data; (—) Equation 3.

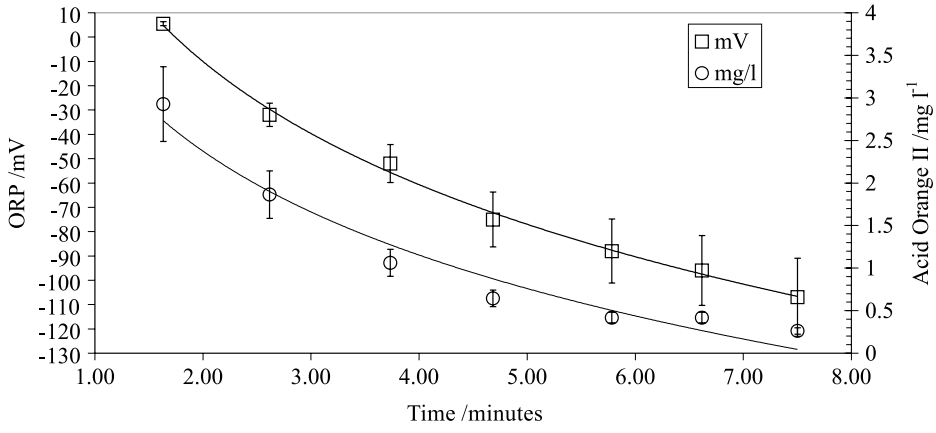

Fig. 2. ORP and dye concentration transients.

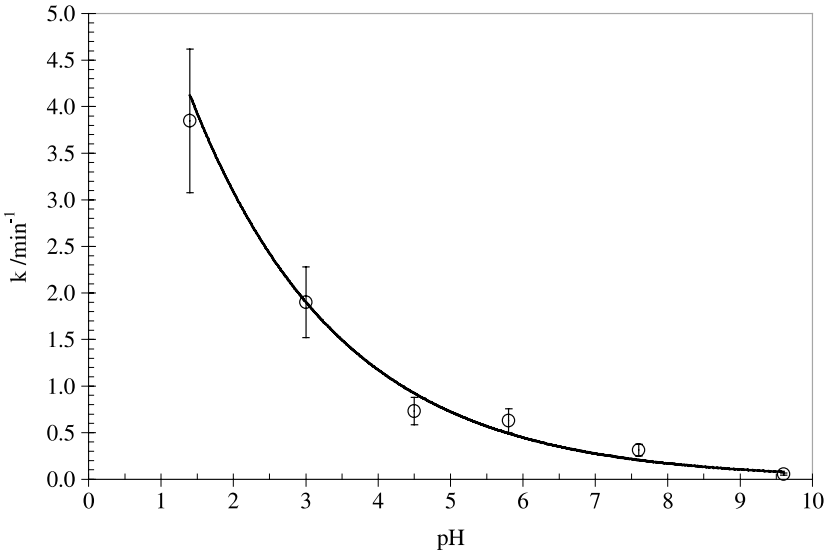

Fig. 4. Effect of pH on pseudo first order reaction rate constant.

Experiments conducted on other matrices and the results arising from these are summarised in Table 4, and Figure 5 shows the location of the experimental conditions when superimposed upon the Pourbaix diagram for iron.

Table 4. E_H, pH and % remediation for range of matrices tested

Run	Contaminant	pH	*E*h* range /mV	% remediation
A	Dye-house concentrate	7.50	+40 to −360	0
B	Pentachlorophenol	6.75	+280 to −680	0
C	Acid Orange II	6.10	+80 to −160	>90
D	Acid Orange II	3.10	+120 to −520	>90
E	Acid Orange II	9.60	+280 to +60	0
F	Acid Blue 113	5.90	+180 to −200	>90

* Standard electrode potential with reference to a standard hydrogen electrode.

4. Discussion

Results indicate that both ORP and dye concentration decay exponentially with reaction time, such that the change in ORP over the course of the remediation reaction is directly proportional to the Acid Orange II concentration (Equation 4). The apparent first order kinetics for dye degradation may reflect upon the electrochemical nature of the remediation reaction, which is driven by anaerobic corrosion whose progress can be monitored by the ORP.

Previous studies of remediation of dyewaste analogues by metallic iron have not reported change in ORP with decolourization [19, 20], although such data have been reported for remediation of halogenated aliphatics and Cr(VI) [21, 22]. However, no correlation of the remediation reaction protaganist concentrations with the ORP shift has been performed, and hence no Nernstian

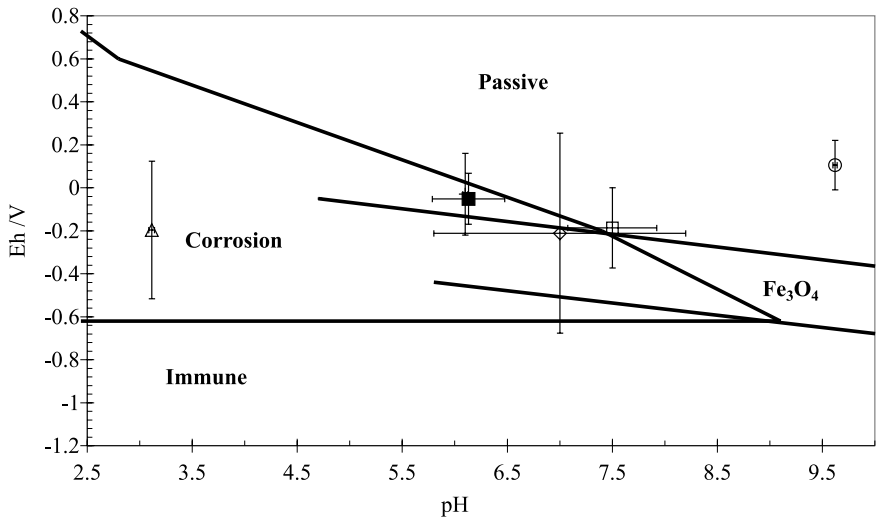

Fig. 5. Experimental conditions for runs (a)–(f) with respect to E_H and pH as depicted on a Pourbaix diagram. Key: (—) Pourbaix, (a) □, (b) ◇, (c) ■, (d) △, (e) ○ and (f) +.

relationship established. The current investigation demonstrates that ORP measurement reproducibly and directly provides the organic contaminant concentration in accordance with classical Nernst theory in the case of Acid Orange II colour remediation.

The relationship between reaction rate and pH is logarithmic (Figure 4), such that the calculated ORP shift (from the Nernst equation) produced by a change in the pH is linearly related to the psuedo first order reaction rate constant k (Figure 6):

$$k(\mathrm{min}^{-1}) = 0.0327\,(\mathrm{mV}) + 3.6018 \qquad R^2 = 0.9668.$$

The HEPES-buffered reaction (potential shift = −75 mV, Figure 6) has a k value slightly below that which would be expected by the ORP shift due to the pH change. This apparent minor anomaly may provide support for claims in the literature that the type of buffer used to adjust the pH affects the reaction rate obtained [23]: HEPES is a biochemical buffer comprising *N*-2 hydroxyethylpiperazine-*N*′-2-ethanesulfonic acid, as opposed to the simpler citric acid/sodium phosphate buffers employed at the other pH values.

According to the Pourbaix diagram, iron dissolution takes place under some of the most acidic conditions employed in this study (i.e., pH 3.1 and an Eh of around −0.2 V); that is, the reaction takes place deep within the corrosion zone. At a pH 6.1 the reaction occurs at the boundary between the corrosion and passivation zone. Raising the pH to 9.6 moves the Eh/pH conditions to entirely within the passivation zone, where a very thin oxide layer impedes corrosion. The reaction rate at pH 3.1 is thus well over an order of magnitude greater than that at pH 9.6 (c.f. Figure 4).

Reaction conditions for the dye concentrate runs fall almost entirely within the passive zone. For PCP, the conditions fall partly in the passive zone and partly within the immune zone (where Fe^0 is the thermodynamically stable phase of iron). Those parts of the PCP and dye concentrate runs where the conditions fall within the favourable corrosion zone are inside the Fe_3O_4 zone (not Fe^{2+}). Fe_3O_4 is insoluble, and so will not flake away from the iron surface but will instead impede contact with the solution. Neither the dye concentrate nor the PCP were remediated by Fe^0 under the conditions investigated. The Pourbaix diagram shows pH and ORP cannot be used in isolation to assess the remediation propensity of a matrix, but must both be employed in conjunction. The logarithmic relationship between pH and reaction rate can then be explained in terms of the zones of the Pourbaix diagram represented by the dashed lines on Figure 4. The steepest part from pH 1.4 to pH 4.5 ($k = -1.0076$ pH + 5.1492, $R^2 = 0.9845$) is where the corrosion zone exists, the moderately steep part of the graph from pH 4.5 to pH 8.0 ($k = -0.138$ pH + 1.3811, $R^2 = 0.9618$) is the part passive-part corrosion zone and the least steep part of the graph coincides with the reaction occurring entirely in the passive zone.

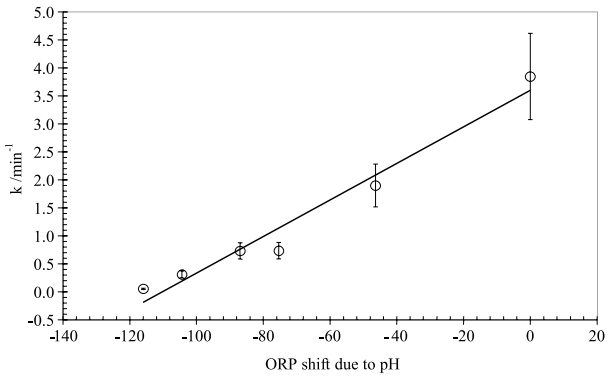

Fig. 6. Pseudo first order rate constant as a function of ORP shift produced by change in pH.

Pourbaix diagrams exist for many metals [24]. Metallic metals, other than iron, have been shown to successfully remediate water contaminants [25]. It seems likely that superimposing Eh and pH conditions for these remediation reactions upon the appropriate Pourbaix diagrams could provide similar insight into the feasibility of those remediation reactions.

5. Conclusions

The study on the remediation of Acid Orange II by reductive degradation with metallic iron has shown that the extent of organics degradation is linearly related to the oxidation reduction potential (ORP). This arises because of the Nernstian relationship governing the concentration of the remediation reaction protagonists, and implies that the progress of the reaction can be monitored on line, on the basis of the ORP reading. Whilst this may not be necessary for a dyewaste, where the reaction progress can be monitored colorimetrically, it is potentially invaluable for contaminants with no UV–visible absorbance band (such as many organic solvents). This would, of course, only apply where side reactions are either negligible or else can be accounted for in some way.

It has further been revealed that the psuedo first order reaction rate constant alters logarithmically with pH and linearly with pH-induced ORP shift. The Eh and pH conditions for successful remediation appear to correlate with zones of Pourbaix diagram where corrosion predominates over passivation. It is postulated that the unsuccessful remediation of PCP may relate entirely to the inappropriate pH and Eh conditions used, and further work is currently being conducted at lower pH levels.

Acknowledgements

This work was sponsored by the Engineering and Physical Sciences Research Council.

References

1. P. Bowden, *Waste and Water Treatment* **32** (1989) 21.
2. A. Ghauch, *Chemsosphere* **43** (2001) 1109.
3. S. Choe, S-H. Lee, Y-Y. Chang, K-Y. Hwang and J. Khim, *Chemosphere* **42** (2001) 367.
4. A. Ghauch, C. Gallet, A. Charef, J. Rima and M. Martin-Bouyer, *Chemosphere* **42** (2001) 419.
5. T. Dombek, E. Dolan, J. Schultz and D. Klarup, *Environmental Pollution* **111** (2001) 21.
6. A. Ghauch and J. Suptil, *Chemosphere* **41** (2000) 1835.
7. W. Feng, D. Nansheng and H. Helin, *Chemosphere* **41** (2000) 1233.
8. A.R. Gavaskar, B.M. Sass, E. Drescher, L. Cumming, D. Giammar and N. Gupta, First International Conference on Remediation of Chlorinated and Recalcitrant Compounds, Vol. **1** (1998), p. 91.
9. R. Muftikian, Q. Fernando and N. Korte, *Wat. Res.* **29** (1995) 2434.
10. F.L. Laque and H.R. Copson, 'Corrosion Resistance of Metals and Alloys' (Reinhold, New York, 2nd edn, 1963).
11. T. Bigg and S.J. Judd, *Environ. Tech.* **21** (2000) 661.
12. T. Bigg and S.J. Judd, *Trans. IChemE Part B*, **79** (2001) 297.
13. P.G. Tratnyek, *Chemistry and Industry*, **July** (1996) 409.
14. J.C. Scully, 'The Fundamentals of Corrosion' (Pergamon, Oxford, 3rd edn, 1990).
15. E.J. Weber and N.L. Wolfe, *Environ. Toxicol. Chem.* **6** (1987) 911.
16. C-P.C. Yen, T.A. Perenich and G.L. Baughman, *Environ. Toxicol. Chem.* **10** (1991) 109.
17. E.J. Weber and R.L. Adams, *Environ. Sci. Technol.* **29** (1995) 1163.
18. J.M. Smolen, E.J. Weber and P.G. Tratnyek, *Environ. Sci. Technol.* **33** (1999) 440.
19. J. Cao, W. Liping, Q. Huang, L. Wang and S. Han, *Chemosphere* **38** (1999) 565.
20. S. Nam and P.G. Tratnyek, *Wat. Res.* **34** (2000) 1837.
21. R.W. Gillham and S.F. O'Hannesin, *Ground Water* **32** (1994) 958.
22. D.W. Blowes, C.J. Ptacek and J.L. Jambor, *Environ. Sci. Technol.* **31** (1997) 3348.
23. D.P. Siantar, C.G. Schreier, C. Chou and M. Reinhard, *Wat. Res.* **30** (1996) 2315.
24. L.L. Shreir, 'Corrosion, 1 Metal/Environment Reactions' (Newnes-Butterworths, London, 1976).
25. T. Boronina, K. Klabunde and G. Segeev, *Environ. Sci. Technol.* **29** (1995) 1511.